MODELING AND EXPERIMENTAL EVALUATION OF THE FACTORS AFFECTING DRILLING FLUID INVASION THROUGH RESERVOIR ROCKS

Alex Tadeu de Almeida Waldmann
PETROBRAS- Cidade Universitária, Q7 – Ilha do Fundão – Prédio 20 – Sala 1017 – Rio de Janeiro - CEP: 21941-598
waldmann.puc@petrobras.com.br

Alex Rodrigues de Andrade
PETROBRAS- Cidade Universitária, Q7 – Ilha do Fundão – Prédio 20 – Sala 1019 – Rio de Janeiro - CEP: 21941-598
alexra.ESTUDANTE@petrobras.com.br

Rosana F.T. Lomba
PETROBRAS- Cidade Universitária, Q7 – Ilha do Fundão – Prédio 20 – Sala 1017 – Rio de Janeiro - CEP: 21941-598
rlomba@petrobras.com.br

André Leibsohn Martins
PETROBRAS- Cidade Universitária, Q7 – Ilha do Fundão – Prédio 20 – Sala 1017 – Rio de Janeiro - CEP: 21941-598
aleibsohn@petrobras.com.br

Paulo Roberto de Souza Mendes
PUC – RIO, Departamento de Engenharia Mecânica - Marquês de São Vicente, 225 – Rio de Janeiro – CEP: 22453 - 900
pmendes@mec.puc-rio.br

Abstract. *This article deals with the understanding of the major operational parameters governing filter cake building drilling fluids invasion through reservoir rocks. Darcy flow modeling of non-compressible cakes proved to reproduce adequately the filtration of a Newtonian fluid + particulate system through ceramic disks. Pressure differential, particle size and shape proved to be relevant parameters affecting filter cake permeability and porosity.*

Keywords: *Drilling fluid, Fluid invasion, Modeling, Reservoir rocks, Particle size distribution*

1. Introduction

Minimizing fluid invasion is a major issue while drilling reservoir rocks. Large invasion may create several problems in sampling reservoir fluids in exploratory wells. Unreliable sampling may lead to wrong reservoir evaluation and, in critical cases, to wrong decisions concerning reservoir exploitability.

Besides, drilling fluid invasion may also provoke irreversible reservoir damage, reducing its initial and /or its long term productivity. Such problem can be critical in heavy oil reservoirs, where oil and filtrate interaction can generate stable emulsions. Invasion in light oil reservoir is less critical due to its good mobility properties (Ladva et al., 2000). Other critical scenario is the low permeability gas reservoirs where imbibition effects may result in deep invasion.

In order to avoid these problems, the drilling fluids industry spends a lot of effort providing non-invasive systems (Reid and Santos, 2003, Luo et al., 2000 among several others). A common practice in the industry is the addition of bridging agents, such as calcium carbonates in the drilling fluid composition. Such products would form a low permeability layer at the well walls which would control invasion. Several authors present fluid composition optimization studies for specific situations (Krilov et al., 2000 among others).

An adequate drilling fluid design requires bridging agent size distribution and concentration optimization. The ability of the fluid system to prevent invasion is normally evaluated by standardized static filtration experiments. In these tests, the fluid is pressurized through a filter paper or into a consolidated inert porous medium. The volume which crosses the porous core is monitored along the time. Santos et al., (1999) presents an experimental study questioning the reliability of filter paper filtration experiments to reproduce invasion into unconsolidated reservoirs.

The main goal of this article is, based on conventional formulation for the standard static filtration experiment, to analyze the impact of several operational parameters which govern invasion, such as: differential pressure between well and reservoir, nature, shape, concentration and particle distribution of the bridging agent, besides rheological behavior of drilling fluid filtrate.

2. Fundamentals

Consider a static filtration experiment, where a fluid, when submitted to constant differential pressure, flows through a porous medium previously saturated with the same fluid. Figure 1 shows the experimental scheme. The fluid

volume that passes over the porous medium is monitored through the time and its rheological properties evaluated at the test temperature.

Considering that the filter cake is incompressible, the collected volume (V) through the time (t) can be obtained, from Darcy law simplified to unidirectional and incompressible flow, by the following expression:

$$t = \left(\frac{h_{pm}}{K_{pm}} \cdot V_L + \frac{V_L^2}{2 \cdot A \cdot K_{fc}} \cdot \left(\frac{C_s}{1 - C_s} \right) \cdot \left(\frac{1}{1 - \phi} \right) \right) \cdot \frac{\mu_f}{\Delta P \cdot A} \quad (1)$$

Where ΔP is the imposed pressure differential, A and h_{pm} are the area and thickness of the porous medium and μ_f is the effective viscosity of the fluid filtrate. K_{pm} and K_{fc} are the permeabilities of the porous medium and filter cake, respectively. Cs is the solids concentration in the fluid, defined as the ratio between the solids volume and total volume (solids volume (Vs) + liquid volume (V_l)). ϕ is the filter cake porosity.

Other hypothesis behind this expression are:

- Filter cake thickness is defined by the solids concentration in the fluid and invasion volume.
- Filter cake permeability is constant.
- Hydrostatic effects are negligible.
- Fluid filtrate presents Newtonian behavior.
- There is no solids invasion into the porous medium.

The complete derivation is detailed in Martins et al., (2004).

3. Experimental work

To evaluate the flow through consolidated porous media, a commercial equipment (FANN - High Pressure High Temperature Press Filter Series 387) was used. In this test, a fixed volume of fluid is set over a synthetic porous medium saturated with the same fluid and submitted to a pre-established pressure differential. The saturation procedure consists in the immersion of the porous medium into the fluid under vacuum conditions. After the saturation stage, the porous medium is placed into the press filter leaned on a high permeability screen in order to minimize the pressure losses in the equipment outlet. Figure 2 shows the experimental cell. Ceramic disks (6.35 cm diameter and 0.635 cm thickness, permeability to air 750 mD and 0.44 v/v porosity) were used as the filtration media.

The porosity was determined using a gas porosimeter. In this technique, a known gas volume under a known pressure is expanded to a chamber that contains the sample. The measured pressure drop is related with the chamber empty volume by the ideal gas law.

The permeability to gaseous fluid was determined in a gas permeameter under a permanent flow pattern. The cylindrical sample is packed in a cell of high or low confining pressure depending on the consolidation rate and a gaseous flow (N2) is established lately. This stabilization is observed and, then, flow and pressure differential readings are taken. The permeability is calculated by Darcy law to compressible fluids. If the sample has a low permeability, a correction is made to the Klinkenberg effect.

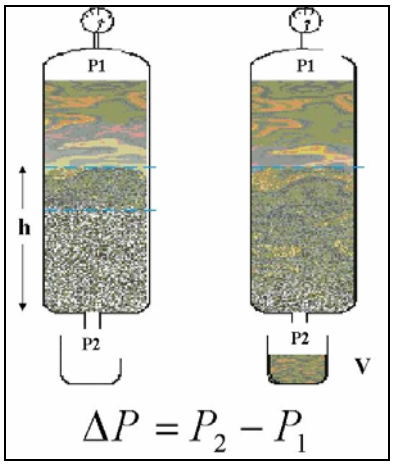

Figure 1 – Filtration scheme submitted to a constant ΔP

Figure 2 –HPHT filtration cell and test apparatus

3.1 Test matrix and procedure

For most tests, unlike in a drilling fluid composition, a Newtonian fluid was adopted as the liquid phase. The reason for that was to avoid any effects on physical properties of the filter cake resultant from the presence of high molecular weight polymers. Such particles, if present in the fluid composition, would certainly affect the dynamic aspects governing filter cake formation.

The Newtonian fluid should be designed in order to avoid premature sedimentation of the solid particles. The system composed by the Newtonian fluid and the bridging agents should be stable during mixing and the filtration test preparation period. Sedimentation should only start when differential pressure is imposed to the system. In order to fulfill such requirements, gravitational sedimentation should start only after there is enough time to start the filtration test. Figure 3 shows the sedimentation curves for water + glycerin systems mixed at different ratios. Figure 4 illustrates the sedimentation experiments for 3.75%v/v (30 lb/bbl) bridging agent concentration. The following volume ratios were used:

- 50/50 v/v glycerin/water
- 60/40 v/v glycerin/water
- 70/30 v/v glycerin/water
- 80/20 v/v glycerin/water

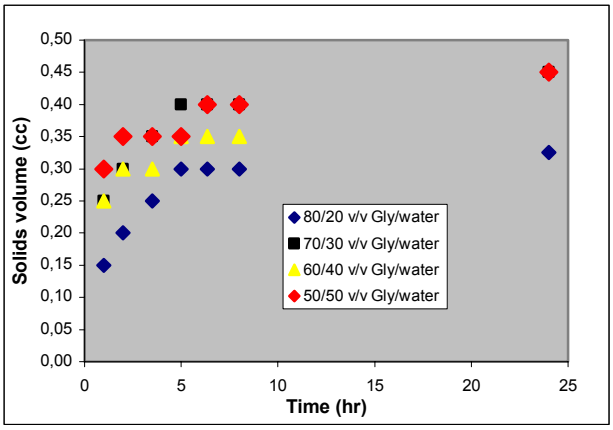

Figure 3 - Sedimentation Curves

Figure 4 - Sedimentation experiments

Due to its adequate suspension capacity, the 80/20 v/v glycerin/water was adopted. The following test matrix was then proposed:

- Fluids: 80/20 v/v glycerin/water and 3 lb/bbl Xhantam gum solution.
- Differential pressure: 40 and 60.
- Bridging agents: Ceramic microspheres and calcium carbonates (flakes and regular).
- Bridging agent concentration : 30 and 50 lb/bbl.

3.2 Characterization of the bridging agents

The characterization of solids size distribution and shape is major issue for filtrate control analysis. One important aspect is that the solid particle should be compatible with the pore throat size distribution of the porous medium: bridging agents should be designed in order not to invade the reservoir rock. Particle shape in sizes distribution will both play important roles in the permoporous properties of the filter cake. Figures 5, 6 and 7 illustrate the shape of the three bridging agents considered in this study, base on their scanning electron microscope (S.E.M) imaging technique. The images highlight the spherical shape of the microspheres and the regular carbonate. The image of the flaked carbonate clearly shows flattened particles. These bridging agents were chosen, among several commercial samples, as the most adequate ones to prevent solids migration trough the porous medium. There is no particle size distribution data available for the flaked carbonate since the technique is not adequate for non – spherical particles. Figures 8 and 9 show the pore size distribution of the ceramic disks experiment. Such analysis was performed using the porosimetry technique. Figures 10 and 11 show the particle size distribution for the ceramic microspheres and regular carbonate, determined by using a particle size distribution analyzer through laser dispersion technique (Malvern – Mastersizer analysis).

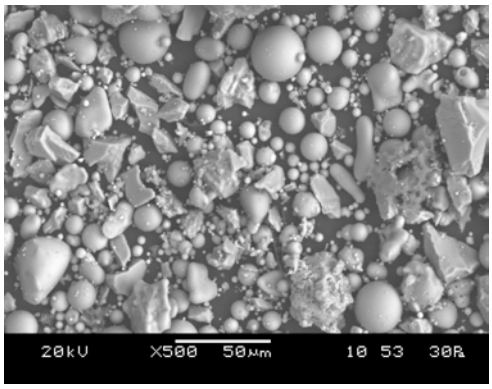

Figure 5 – Ceramic microspheres

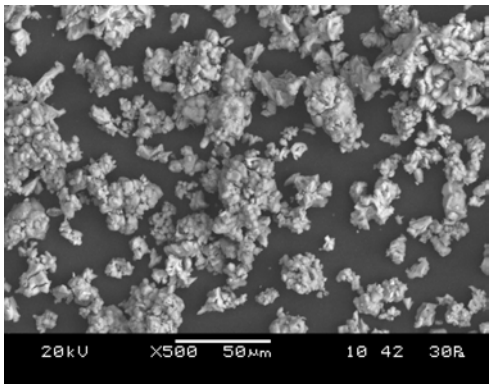

Figure 6 – Regular carbonate

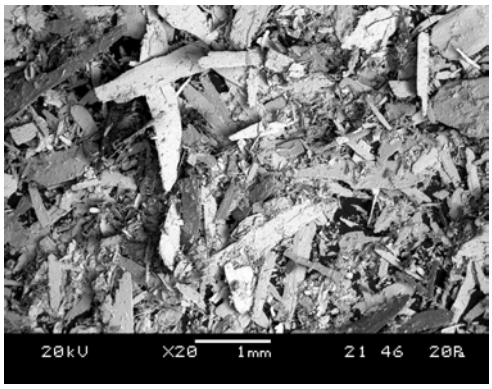

Figure 7 – Flaked carbonate

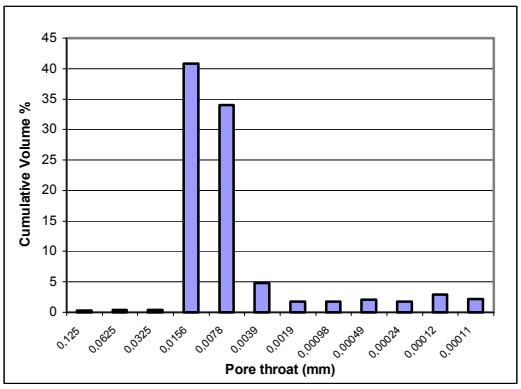

Figure 8 - Pore size distribution of the ceramic disk

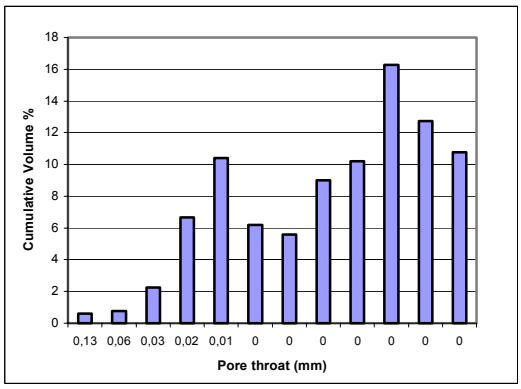

Figure 9- Pore size distribution of the ceramic disk

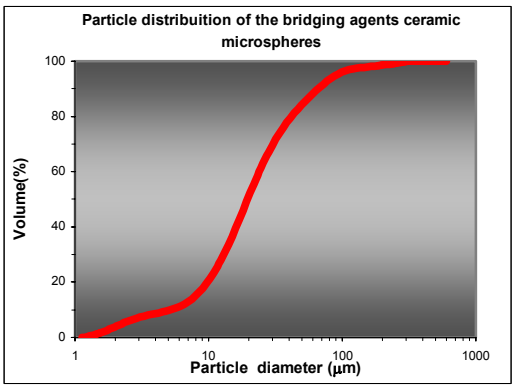

Figure 10 - Particle distribution of the bridging agent – Ceramic microspheres

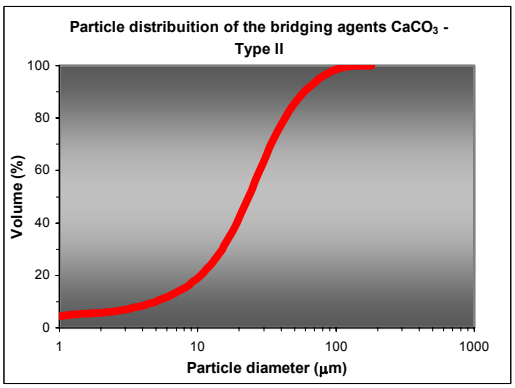

Figure 11 - Particle distribution of the bridging agent – Regular carbonate

3.3 Experimental procedure

- The Newtonian fluid without solids is displaced through the porous medium previously saturated with the same fluid to determine its original permeability to the liquid. The fluid flow rate which crosses the porous medium at each pressure differential (40, 60, and 80 psi) is measured as well as the viscosity at the same temperature of the test.
- The test fluid (containing the bridging agent) is displaced at a fixed pressure differential with flow, rheological properties and density being evaluated at the test temperature. Filter cake permeability is then estimated through Equation 1.
- After the filtration process is concluded, the equipment is disassembled and porous medium + filter cake system removed (M_1). The system is weighted and its thickness evaluated (h_{cake}). The system is then repositioned into de filtration cell where it is submitted to the flow of water. After this process, the system, now saturated with water, is removed and weighted again (M_2). Filter cake porosity is evaluated based on Equation 2.

- The filter cake is now removed from the surface of the porous medium. New Newtonian fluid (without solids) displacement through the porous medium at same pressure differentials used in first step. The objective is to check if there was permeability reduction after the test fluid flow.

$$\phi_{Cake} = \frac{\dfrac{M_1 - M_2}{(\rho_{Gly} - \rho_{H_2O})} - V_{Disk\ Porous}}{V_{cake}} \tag{2}$$

4. Results

Table 1 summarizes the tests results. The ability of the bridging agents to minimize fluid invasion will be captured by the filter cake's permeability and thickness. Filter cake porosity when available and permeability impairment of the porous media (indicating eventual solids invasion) are also detailed. The correlation coefficient reflects the adequacy of the non-compressible filter cake approach to fit experimental data. For all the cases the hypothesis seemed reasonable. Figures 12, 13 and 14 show the comparison between the measured and estimated volumes as functions of the filtration time for tests with the 3 bridging agents. A sensibility analysis on the effect of the governing parameter follows. Each test was performed 3 times aiming repeatability.

Table 1. Tests results

K_{after} (mD)	K_{before} (mD)	ΔP	Conc.	Bridging Agents	K_{Cake} (mD)	h (cm)	ϕ	R
696	622	40 PSI	50 lb/bbl	Ceramic microspheres	181	1.4	N/A	0.99
792	789	60 PSI	50 lb/bbl	Ceramic microspheres	106	1.5	N/A	0.99
808	818	60 PSI	50 lb/bbl	Ceramic microspheres	97	1.5	N/A	0.99
492	451	60 PSI	30 lb/bbl	Ceramic microspheres	49	1.2	N/A	0.99
580	455	60 PSI	30 lb/bbl	Ceramic microspheres	38	1.7	N/A	0.99
614	513	60 PSI	30 lb/bbl	Ceramic microspheres	33	1.1	N/A	0.99
534	526	60 PSI	30 lb/bbl	Ceramic microspheres	21	0.9	N/A	0.99
780	795	40 PSI	30 lb/bbl	Ceramic microspheres	49	0.5	N/A	0.98
725	784	40 PSI	30 lb/bbl	Ceramic microspheres	44	0.9	N/A	0.99
754	764	40 PSI	30 lb/bbl	Ceramic microspheres	50	1.0	0.57	0.99
727	733	40 PSI	30 lb/bbl	Ceramic microspheres	55	1.2	0.52	0.98
824	813	40 PSI	30 lb/bbl	Flaked carbonate	36	2.0	N/A	0.99
574	488	40 PSI	30 lb/bbl	Flaked carbonate	33	1.5	N/A	0.98
876	780	40 PSI	30 lb/bbl	Flaked carbonate	32	1.9	N/A	0.98
658	636	40 PSI	30 lb/bbl	Flaked carbonate	21	-	N/A	0.99
780	755	60 PSI	30 lb/bbl	Flaked carbonate	36	1.5	N/A	0.99
608	613	60 PSI	30 lb/bbl	Flaked carbonate	30	1.5	N/A	0.99
543	651	60 PSI	30 lb/bbl	Flaked carbonate	29	1.5	N/A	0.99
707	734	60 PSI	50 lb/bbl	Flaked carbonate	38	3.2	N/A	0.99
684	583	60 PSI	50 lb/bbl	Flaked carbonate	38	3.5	N/A	0.99
784	745	60 PSI	50 lb/bbl	Flaked carbonate	51	-	N/A	0.97
845	795	40 PSI	30 lb/bbl	Regular carbonate	91	1.2	0.53	0.98
777	795	40 PSI	30 lb/bbl	Regular carbonate	117	1.3	0.51	0.99
793	784	40 PSI	30 lb/bbl	Regular carbonate	117	1.2	0.52	0.99
730	728	40 PSI	30 lb/bbl	Regular carbonate	96	1.2	0.58	0.99
682	678	60 PSI	50 lb/bbl	Regular carbonate	131	2.3	0.65	0.99
475	572	60 PSI	50 lb/bbl	Regular carbonate	97	2.6	0.63	0.98
450	478	60 PSI	50 lb/bbl	Regular carbonate	72	2.4	0.61	0.99
779	478	60 PSI	50 lb/bbl	Regular carbonate	106	2.5	0.79	0.99
389	317	60 PSI	30 lb/bbl	Regular carbonate	91	1.7	0.67	0.99
687	638	60 PSI	30 lb/bbl	Regular carbonate	138	1.8	0.61	0.98
657	544	60 PSI	30 lb/bbl	Regular carbonate	44	1.8	0.55	0.99

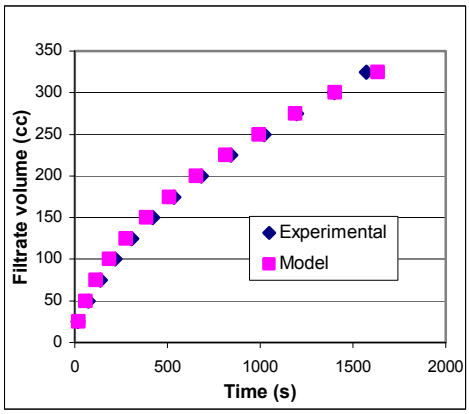

Figure 12 – Ceramic microspheres

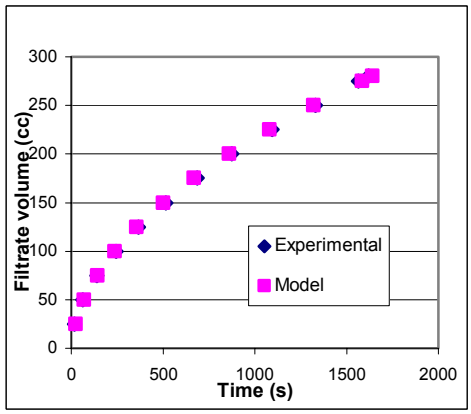

Figure 13 – Flaked carbonate

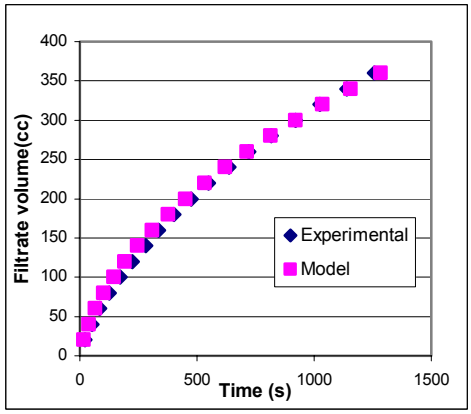

Figure 14 – Regular carbonate

- Pressure Differential. Figures 15, 16 and 17 show the effect of the imposed differential pressure on the filter cake permeability for the 3 different bridging agents. For all the cases, as expected, the permeability decreased with the increase of differential pressure. Further data are required to explore the wider range of pressure differentials which characterize drilling operations.

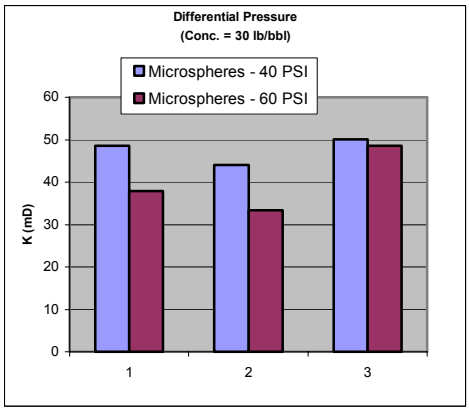

Figure 15 - Effect of ΔP – Microspheres

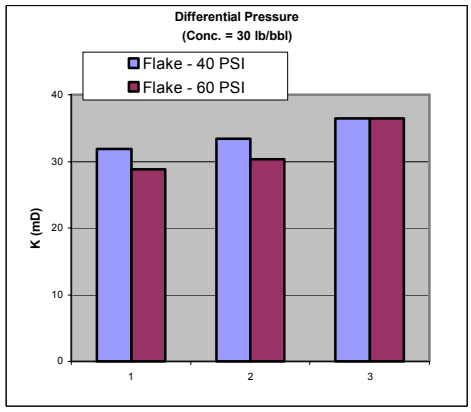

Figure 16 – Effect of ΔP – Flaked carbonate

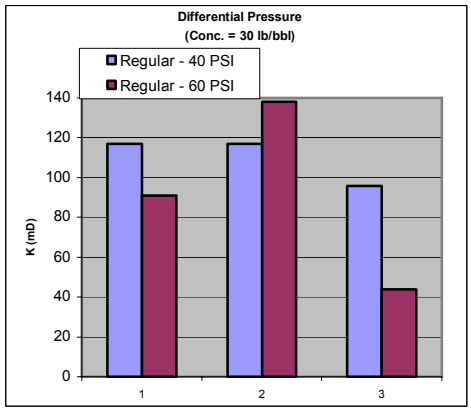

Figure 17 - Effect of ΔP – Regular carbonate

- Nature and shape of the bridging agent: Figures 18, 19 and 20 illustrate filter cake permeabilities for the 3 different bridging agents at two pressure differentials and concentrations. Results indicate that particle shape plays an important role on filter cake permeability reduction. In both situations, the flaked particle resulted in lower filter cake permeabilities, probably to particle accommodation. Effects of particle size distribution certainly play a role in the process and require further investigation.

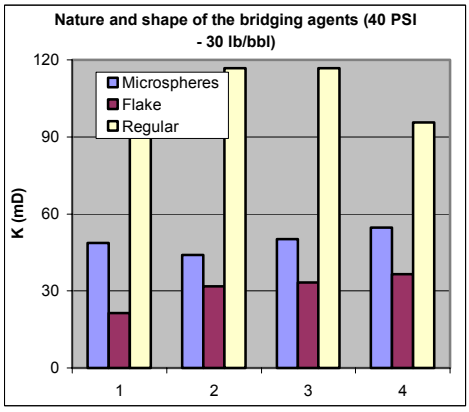

Figure 18 -Effect of shape - 40psi /30lb/bbl

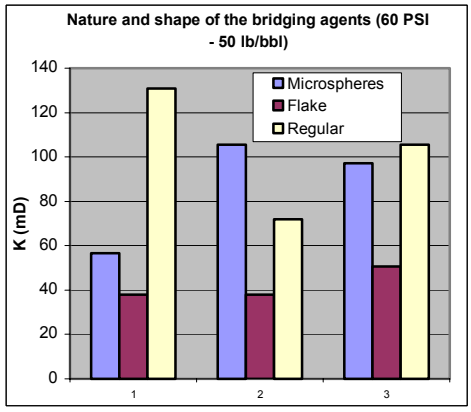

Figure 19 -Effect of shape - 60psi /50lb/bbl

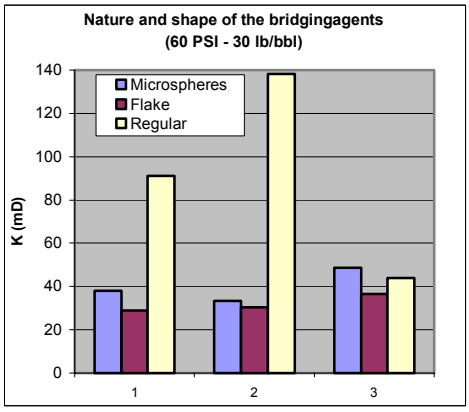

Figure 20- Effect of shape – 60psi /30lb/bbl

- Bridging agent concentration: Figures 21, 22 and 23 show the effect of solids concentration on the filter cake permeability. For the flaked particle, the increase of solids concentration helped to reduce filter cake permeability. Such effect was negligible for the ceramic microspheres.

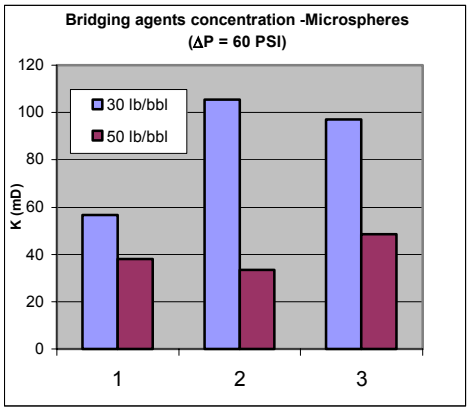

Figure 21 – Effect of conc. - Microspheres

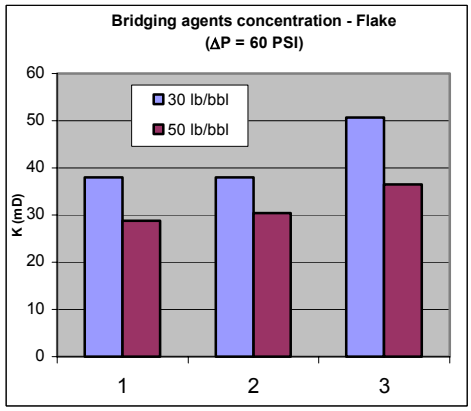

Figure 22 - Effect of conc.– Flaked carbonate

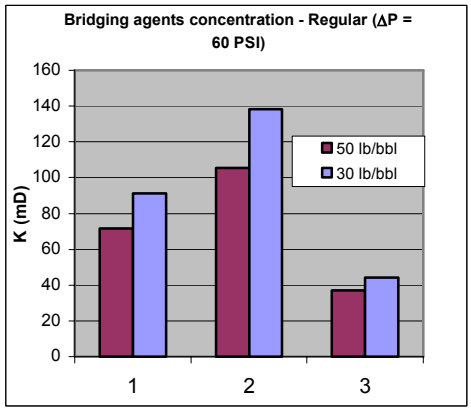

Figure 23 - Effect of conc.– Regular carbonate

- Fluid nature. Preliminary exploratory tests were run with xhantam gum solutions as liquid phases. A first and important conclusion is that the presence of polymers can generate compressible filter cakes. This fact can be exemplified by Fig. 24 where model results don't match the experiment.

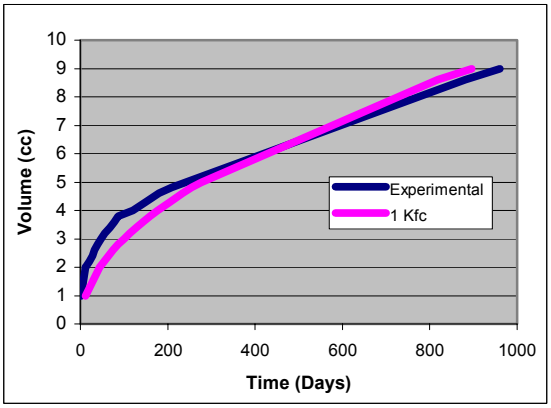

Figure 24 - Linear model validation

5. Final Remarks

- A sensibility analysis on the linear Darcy flow of a cake building Newtonian fluid through porous media indicates that filter cake permeability is a major parameter governing the process.
- The experimental procedure proposed in this article is a comprehensive methodology for the determination of drilling filter cake properties which govern fluid invasion through reservoir rocks (permeability and porosity).
- Effects of Pressure differential, particle shape, size and concentration on filtration are illustrated in the article. The choice of a Newtonian fluid as the continuum media generated non-compressible cakes at low differential pressures. High differential pressures and non Newtonian fluids can generate compressible cakes with higher sealing capacity.
- Further steps in the study include the determination of optimum particle size distribution which minimizes filter cake permeability, modeling of compressible cake formation and testing real fluid systems. Model results indicate that filter cake permeability is the major factor governing invasion. Several efforts can be made regarding fluid composition in order to optimize this parameter. Solids size and shape can be a good path for that.

6. References

KRILOV, Z., DOMITROVIC, D., SORIC, T. and GRACANIN, M.: "Drill-In Fluid Selection for High-Temperature, Sour Gas, Naturally Fractured Reservoirs", paper presented at the 2000 SPE International Petroleum Conference and Exhibition, Villahermosa, Mexico, 1-3 February.

LADVA, H.K.J., TARDY, P., HOWARD, P.R. and DUSSAN V., E.B.: "Multiphase Flow and Drilling-Fluid Filtrate Effects on the Onset of Production", paper presented at the 2000 SPE International Symposium on Formation Damage Control, Laffayete, Louisiana, 23-24 February.

LUO, S., Li, Y., MENG, Y., ZHANG L.: "A New Drilling Fluid for Formation Damage Control Used in Underbalanced Drilling", paper presented at the 2000 IADC/SPE Drilling Conference, New Orleans, Louisiana, 23-25 February.

MARTINS, A. L, WALDMANN, A. T. A., ARAGÃO, A. F. L. and LOMBA, R. F. T.: "Predicting and Monitoring Fluid Invasion in Exploratory Drilling", paper presented at the 2004 SPE International Symposium and Exhibition on Formation Damage Control, held in Lafayette, Louisiana, U.S.A., 18–20 February 2004.

REID, P. and SANTOS, H.: "Novel Drilling, Completion and Workover Fluids for Depleted Zones: Avoiding Losses, Formation Damage and Stuck Pipe", paper presented at the 2003 SPE/IADC Middle East Drilling Technology Conference & Exhibition, Abu Dhabi, UAE, 20-22 October.

SANTOS, H., VILLAS-BOAS, M.B., LOMBA, R.F.T., SÁ, C.H.M., OLIVEIRA, S.F. and Costa, J.F.: "API Filtrate and Drilling Fluid Invasion: Is There Any Correlation?", paper presented at the 1999 Latin American and Caribbean Petroleum Engineering Conference, Caracas, Venezuela, 21-23 April.